SF2A 2006
D. Barret, F. Casoli, T. Contini, G. Lagache, A. Lecavelier, and L. Pagani (eds)

MAGNETIC INSTABILITIES IN STELLAR RADIATION ZONES

A.S. Brun[1,2] and J.-P. Zahn[2]

Abstract. Using the 3-dimensional ASH code, we have studied numerically the instabilities that occur in stellar radiation zones in presence of large-scale magnetic fields and differential rotation. We confirm that some configurations are linearly unstable, as predicted by Tayler and collaborators, and we determine the saturation level of the instability. However we found no sign of the dynamo mechanism suggested recently by Spruit.

1 Introduction

Large scale magnetic fields are prone to linear instabilities, which have been studied in detail by Tayler and his collaborators (Tayler 1973, Markey & Tayler 1973, 1974; Tayler 1980; Pitts & Tayler 1985) and by Wright (1973). These instabilities have been reviewed recently by Spruit (1999, 2002), who suggests that a fossil magnetic field permeating the radiation zone of a rotating star can even trigger a dynamo mechanism, and maintain a level of turbulence that causes the mixing of chemical elements. A crucial point in the description of this mechanism is to determine the saturation level of the field in the non-linear regime, and to verify whether the field is regenerated; this lies beyond analytical treatment and can only be achieved through numerical simulations.

We have carried out such simulations for the primary purpose of checking whether a fossil magnetic field can prevent the radiative spread of the solar tachocline, as was claimed by Gough and McIntyre (1998). But since we used a three-dimensional code, we were able to capture also the Tayler instabilities, which are genuinely non-axisymmetric, and to study them in the non-linear phase of their growth (Brun & Zahn 2006). In Brun & Zahn (2006) we have seen the development of the Tayler instabilities in presence of rotation and of a latitudinal shear imposed at the top of the tachocline. Here we report the results of a more recent numerical study, in which we have computed non rotating and rotating models of the solar radiative zone, but without imposing the latitudinal shear as in the tachocline runs.

2 The Numerical Model

We make use of the hydrodynamic ASH code (Anelastic Spherical Harmonic; see Clune et al. 1999; Miesch et al. 2000; Brun & Toomre 2002) which was originally designed to model the solar convection zone. It has since been extended to include the magnetic induction equation and the feedback of the field on the flow via Lorentz forces and Ohmic heating (see Brun, Miesch & Toomre 2004 for more details). This code solves the full set of 3–D MHD anelastic equations of motion (Glatzmaier 1984) in a rotating spherical shell on massively-parallel computer architectures.

Here we apply it to examine the nonlinear evolution of Tayler's non axisymmetric instabilities in the presence or absence of rotation and of a latitudinal shear. The computational domain extends from $r_{\rm bot} = 0.35\,R_\odot$ to $r_{\rm top} = R = 0.72\,R_\odot$ ($R_\odot$ is the solar radius); we thus focus on the bulk of the stably stratified zone, excluding the nuclear central region, and we ignore its possible back reaction on the convective envelope. We refer the reader to Brun and Zahn (2006) for further information on the equations that are solved, their boundary conditions and the numerical method employed. To enable us to resolve the smallest scales, the diffusion coefficients

[1] DSM/DAPNIA/Service d'Astrophysique, CEA/Saclay, 91191 Gif-sur-Yvette, France; AIM, UMR 7158, CEA - CNRS - Université Paris VII
[2] LUTH, Observatoire de Paris, 5 place Jules Janssen, 92195 Meudon, France

(viscosity, thermal and magnetic diffusivities) were all increased with respect to their solar values, but we took care to respect their hierarchy. The time-step was chosen such as to accommodate the Alfvén crossing time. In the cases discussed here, we imposed initially a purely poloidal field of dipolar type, which was buried below $r_{\rm bot} = 0.64\, R_\odot$; its strength of about 3 kG was taken so that the magnetic torque could balance the advection of angular momentum through the tachocline circulation (cf. Brun & Zahn 2006).

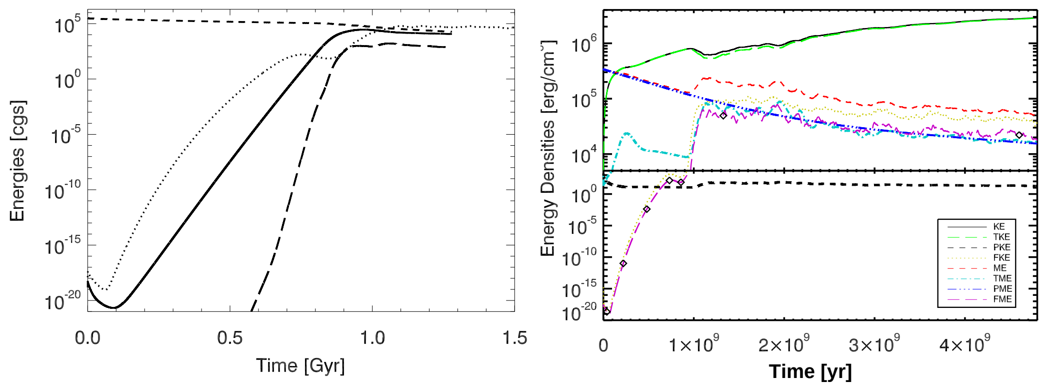

Fig. 1. Left Panel: Temporal evolution of the magnetic energies in the absence of rotation and shear. Note the fast growth of FME (solid curve), the decrease of ME (dash), and the rapid (but delayed) rise of TME (long dash). To ease the comparison with the right panel, we have superimposed the FME curve of the tachocline case (here represented as a dotted line). Right panel: Temporal evolution of kinetic and magnetic energies in the presence of rotation and shear. We clearly see the 2 phases of non-axisymmetric instability (characterized by the fast increase of FKE and FME): the first, for $t < 1$ Gyr, is associated with the unstable configuration of the purely dipolar initial field, and the second, for $t > 1$ Gyr, with the toroidal field produced by winding up the poloidal field through the differential rotation. The time is given in solar equivalent units, i.e. rescaled by the ratio $t_{\rm ES}({\rm Sun})/t_{\rm ES}({\rm simulation})$.

3 Non Axisymmetric Instabilities in Radiative Zone

The instabilities are best described in following the temporal evolution of various components of the kinetic (KE) and magnetic (ME) energies, averaged over the whole computational domain (see Fig. 1). PKE & PME designate the mean (axisymmetric) poloidal components of respectively KE and ME, TKE & TME their mean toroidal components, and FKE & FME their non-axisymmetric components (see Brun et al. 2004 for their analytic expressions). To facilitate the comparison with the Sun, the time is given in solar equivalent units, i.e. rescaled by the ratio $t_{\rm ES}({\rm Sun})/t_{\rm ES}({\rm simulation})$, where $t_{\rm ES} = (N/\Omega)^2(R^2/\kappa)$ is the Eddington-Sweet time (N: buoyancy frequency, Ω: angular velocity, κ: thermal diffusivity).

In the left panel of Figure 1, we represent ME, FME, and TME for the non rotating case. We clearly see the fast, exponential growth of FME by more than 20 orders of magnitude (the e-folding time is ≈ 13.5 Myr) and its nonlinear saturation around 900 Myr at about the amplitude that ME (and PME not shown) have reached, since contrary to FME, ME is decaying on a slow Ohmic time scale. Further we note that ME starts decaying faster at the very moment of the saturation of FME. This could be interpreted as evidence for a turbulent enhancement of the magnetic diffusivity. The toroidal mean magnetic energy TME, rises from an extremely tiny value with a growth rate about twice faster compared to FME (the e-folding time is ≈ 6.5 Myr). The fluctuations are first located at low latitude and at the bottom of the domain (see Fig. 2 top left). We conclude that it is one of the instabilities described in the pioneering works quoted above, which occurs when the field is purely poloidal. When analyzing the energy spectrum in m of the fluctuations of the azimuthal field B_ϕ, one sees clearly that the maximum growth occurs at rather high azimuthal wavenumber: $m \approx 20$. This is in reasonable agreement with Wright (1973) and Markey & Tayler (1974), who found that the growth-rate should steadily increase with m in the non-dissipative case. No mean toroidal field is produced in the unstable region, presumably because the magnetic helicity was initially zero. Quickly after, the instability starts filling up the whole sphere (Fig. 2 top middle and top right), and progressively the maximum amplitude of the spectra shifts toward lower m and ℓ as the dissipation of the smallest scales starts kicking in. Note in the middle panel of the top row of Figure 2, how the instability develops, by having patches of positive and negative polarity starting to rotate and entrain one another, not unlike interchange instabilities. However we do not see a dynamo process in this simulation, since all the magnetic components of the magnetic fields end up decaying away.

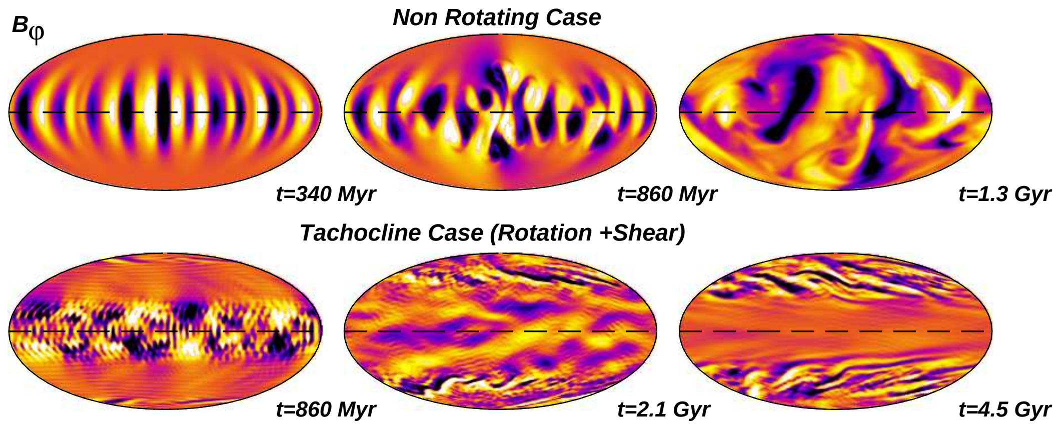

Fig. 2. Temporal evolution near the base of the domain of the non axisymmetric longitudinal field (azimuthal average (m=0) has been subtracted) for the non rotating case and for the tachocline case with rotation and shear. Note how the nonlinear evolution of the instability differs in the presence of large scale shear, with B_ϕ taking a ribbon like shape.

We now turn to the tachocline case by looking at the right panel of Fig. 1 that represents all the components of ME and KE, not just a subset as in the left panel. From the onset, as in the previous case, starting from an extremely weak non-axisymmetric velocity field, FKE & FME rise exponentially by many orders of magnitude at a fast pace (the e-folding time is ≈ 10 Myr). They saturate around 700 Myr at a level which is, contrary to the previous case, 1000 times below the energy of the mean poloidal field (PME). The fluctuations are located at low latitude and at the bottom of the domain (Fig. 2 bottom left); when analyzing the energy spectrum in m of the fluctuations of the azimuthal field B_ϕ, one sees clearly that the maximum growth occurs at rather high azimuthal wavenumber: $m \approx 40$. Here the presence of rotation seems to favour even higher m than in the non rotating case. However the instability of the initial poloidal field is not delayed by the rotation and possesses a faster growth rate. This is surprising because rotation should decrease the growth rate compared to a non rotating case. It is possible that the presence of a large scale shear in which the weak poloidal field at the pole quickly connect to, provide more energy for the development of the instability that when the outer boundary is immobile. To check this hypothesis we are currently computing the purely rotating case and indeed it seems that the growth rate of FME in the rotating case is slower than in the non rotating one, which is in qualitative agreement with Pitts & Tayler (1985). Thus the presence of shear in the tachocline case is clearly modifying the nonlinear development of the instability.

Indeed we can note the appearance of two bands of toroidal field of opposite polarity in the upper part of the domain (see Fig. 2 bottom/middle), one at mid latitude and the other close to the rotation axis, with opposite sign in each hemisphere. This field is generated by the shearing of the poloidal field, which very soon encountered the differential rotation spreading down from the convection zone. At about 1.2 Gyr the energy TME, averaged over the whole domain, matches that of the mean poloidal field, meaning that locally the toroidal field can be much stronger than the poloidal field, since it occupies a smaller volume. That toroidal field is unstable to low m perturbations, with the strongest component at $m = 1$, as predicted by the theory. Note that the mean toroidal field and the associated instability draw their energy from the differential rotation, as indicated by the conspicuous inflection of the TKE curve in Fig. 1b, at 1.1 Gyr. Clearly the presence of a strong differential rotation modifies the nonlinear evolution of the magnetic field and its topology. In this case the magnetic field finally organise itself into ribbon like structures near the poles due to the strong and continuous ω-effect present in these region. This is in sharp contrast with the previous case, where no preferred axes are present (except the initial magnetic axis of the seed poloidal field, which does not seem to play any significant role), and the instability develops over the entire sphere.

Thereafter all energies but one slowly decline, at a rate which is controlled mainly by the Ohmic dissipation of the mean poloidal field (PME): in our rescaled solar units, the e-folding time would be $R^2/2\pi^2\eta \approx 2$ Gyr for a uniform motionless sphere (Cowling 1957), which is compatible with what we see here. The decay of that field is particularly smooth, and there is no sign that it is regenerated or even affected by the instability. The mean toroidal field accompanies closely the decline of the mean poloidal field (see Fig. 1b and Fig. 2 bottom right), and so do the non-axisymmetric components FKE and FME, with the kinetic energy in these perturbations being about twice their magnetic energy. In the tachocline case the only exception to that overall decline is the mean toroidal kinetic energy TKE, which steadily increases as the differential rotation spreads deeper and to lower latitudes. The kinetic energy of the meridional flow (PKE) is the smallest of all energies; it is mostly concentrated toward the top of the domain and it remains almost constant during the whole evolution.

4 Conclusion

Since we used a three-dimensional code, we were able to observe the non-axisymmetric instabilities associated with our field configurations. In the early phase, they occur in a narrow equatorial belt at the base of the computational domain, and they are due to the purely poloidal field we have imposed initially. Later on, depending on whether there is or not a large scale shear present in the radiative stale zone, they are present either at all depths near the poles, where the shear of the differential rotation, which has spread from the top of the radiation zone, keeps generating a strong toroidal field or throughout the sphere with no latitudinal preference and a much less organized parity antisymmetry or favored direction. Their properties agree reasonably well with the predictions of Tayler and his collaborators, which were recently reviewed and completed by Spruit (1999, 2002). However the presence of shear seems to modify the growth rate and nonlinear evolution of the instability more than the rotation alone.

An important result of our simulations is that these instabilities do not interfere with the mean poloidal field; they are able to distort the “isogyres” (surfaces of constant angular velocity Ω), thus affecting somewhat the production of the toroidal field, but even there they seem to have limited impact. Thus we do not see a dynamo process occurring in our simulated radiative interior, as was suggested by Spruit: in all cases studied the mean poloidal field is not regenerated but it decays away through Ohmic diffusion. However it is possible that the magnetic Reynolds number required to trigger the dynamo mechanism is beyond that achieved in our simulations. More simulations are under way to test the influence of the magnetic diffusivity (or equivalently the effective magnetic Reynolds number of the simulation) on the development of the instability, its saturation level and the presence or not of a dynamo in stellar radiative zone.

We thank the CEA/CCRT and the CNRS/IDRIS supercomputer centers for letting us use their resources.

References

Brun, A. S., Miesch, M. S., & Toomre, J. 2004, ApJ, 614, 1073
Brun, A. S., & Toomre, J. 2002, ApJ, 570, 865
Brun, A. S., & Zahn, J.-P., A&A, 457, 657
Clune, T. L., Elliott, J. R., Glatzmaier, G. A., Miesch, M. S., & Toomre, J. 1999, Parallel Comput., 25, 361
Cowling, T. G. 1957, Magnetohydrodynamics (New York: Interscience Publ.)
Glatzmaier, G. A. 1984, J. Comp. Phys., 55, 461
Gough, D. O., & McIntyre, M. E. 1998, Nature, 394, 755
Markey, P., & Tayler, R. J. 1973, MNRAS, 163, 77
Markey, P., & Tayler, R. J. 1974, MNRAS, 168, 505
Miesch, M. S., Elliott, J. R., Toomre, J., Clune, T. L., Glatzmaier, G. A., & Gilman, P. A. 2000, ApJ, 532, 593
Pitts, E., & Tayler, R. J. 1985, MNRAS, 216, 139
Spruit, H. C. 1999, A&A, 349, 189
Spruit, H. C. 2002, A&A, 381, 923
Tayler, R. J. 1973, MNRAS, 161, 365
Tayler, R. J. 1980, MNRAS, 191, 151
Wright, G. A. E. 1973, MNRAS, 162, 339